Journal of Korean Association of Crystal Growth
Vol. 7, No. 4 (1997) 599-609

Analysis of microstructural evolutions during advanced ceramics processing : I. Phase behavior of colloidal dispersion

Hern Kim
Department of Chemical Engineering, Myong Ji University, Yongin 449-728, Korea

세라믹 제조시 미세구조 변화의 해석 : I. 콜로이드 분산의 상거동

김 헌
명지대학교 화학공학과, 용인, 449-728

Abstract The phase behavior and dynamics of colloid suspensions and the resulting structures and properties of powder compacts were examined by a computer experimental method for cooperative packing processes. A wide range of properties and process conditions such as arbitrary particle size, medium densities, field strength, and temperature could be examined using the Peclet number (Pe). We demonstrated that an optimum range of Peclet number for the ordering of sediments was present and that the phenomena related to the ordering such as the onset of crystallization, the phase behavior, etc. strongly depend on process conditions. The present work appears to be useful to design the processing method of ceramic spherical submicron powders for the preparation of high-density green compacts.

요 약 콜로이드 분산의 상거동 및 동적 운동 및 형성되는 침적체의 구조와 물성은 전산실험법으로 조사되었다. 다양한 물성과 공정조건들은 Peclet수를 사용하여 조사될 수 있다. 형성된 구조는 구조인자 및 반경방향 분포함수로서, 물성은 계면의 궤적선도를 사용하여 조사되었다. 침적체의 형성 조건과 구조가 조사되었으며 침적시간과 높이에 따른 구조와 물성이 조사되었다. 침적체가 결정구조를 갖는 최적 Peclet수의 범위가 있으며 결정화와 관련된 현상들은 공

정조건에 크게 좌우됨을 알 수 있다. 현 방법과 결과들은 고밀도 침적체의 제조시 세라믹 미분체 공정을 설계하는데 사용될 수 있다.

1. Introduction

Colloidal interaction plays a critical role in determining the equilibrium structures of dense dispersions used in colloidal processing of ceramics. In addition, the dynamic aspects of structural evolution and their impact on the final microstructure obtained during processing are so crucial [1]. The microstructure of the green body has a strong influence on the densification of the specimen during sintering and on the corresponding changes in the defect and void structures in the final specimen [2]. For example, the use of monodisperse spherical submicron powders for the preparation of ideal high-density green bodies which can subsequently be densified at relatively lower temperatures has been the subject of considerable research in the past decade. These ordered compacts with high coordination numbers and very uniform pore size distributions are capable of densifying uniformly with the abnormal grain growth [3,4]. Thus it should be possible to prepare full-density submicron-grain-size ceramics by densifying these compacts at temperatures several hundred degrees lower than their counterpart.

Colloidal phenomena are influenced by a number of interparticle interactions such as van der Waals attraction, steric and electrostatic repulsions, Brownian motion and hydrodynamic forces [5]. From typical experiments on colloidal systems it has been observed that these forces act cooperatively to determine the structures of the dispersions. The relative importance of these forces is determined by the characteristics of the particulate systems considered and the physicochemical conditions during powder processing. Recently, sedimentation of colloidal particles governed by both Brownian motion and gravity without any attraction between particles has received considerable attention, since *colloidal systems show a disorder-order* transition similar to that of molecular system under the influence of the above forces [6,7], and also since such systems can be useful in the production of advanced ceramics [8,9]. In addition, it has been noted [10] that the influence of such factors on the structures and properties of colloid dispersions and their resulting sediments can be effectively examined in terms of Peclet number, which determines the relative importance of gravitational and Brownian forces.

In many recent experiments [11,12] coated silica particles in the nanometer-size range dispersed in cyclohexane have been used as model hard spheres. It has been observed that an ordered structure is formed under appropriate conditions as the colloidal particles sediment.

The formation of ordered structures depends on the initial volume fraction, the particle size, etc. Experimental studies of these phenomena usually require special facilities for detecting the phases and phase boundaries (e.g., X-ray, neutron and light scattering, among others) and additional expensive instrumentation for particle characterization. Moreover, such experiments also require more than several days for completion and for obtaining reliable data. On the other hand, computer simulations are relatively simple and, if used properly and judiciously, can offer considerable insights more easily and at less cost. Some computer simulations are available in the literature, for studying the phase behavior of hard spheres (such as glass transition or melting [13,14]), but those available are not adequate for applications related to sedimentation or deposition phenomena relevant in ceramic powder processing. One should also note here that theoretical studies, e.g., for the sedimentation of noncolloidal particles [15], can provide information about phase boundaries and their dynamics through examinations of the variation of volume fraction with height, etc., but are not sufficient for providing information on local and global variations of phase themselves. Computer simulations thus serve as an attractive adjunct to experimental and theoretical approaches, particularly in the case of cooperative packing (or deposition) processes.

The purpose of the present work is to study the dynamic phase behavior in the settling colloidal dispersion, whose sediments show an ordering in the structures. In order to get some insights about the evolution of structure in a settling dispersion and in the resulting sediments and about the dynamics of individual particles, we examine how a dispersion of particles forms a concentrated deposit and how the structure of the sediment changes via cooperative interactions among the particles. In particular, the phase behavior of a sedimentation process as a function of sedimentation time and the depth of the dispersion is examined.

2. Computer Experiment

2.1. Simulation Procedure

In this simulation, the volume containing the particles is defined by a vertical strip of width L and an initial height of H_0. First, the particles are randomly placed in the given volume, without overlapping. The particles are then moved one at a time with a small displacement $\{\Delta x, \Delta y\}$ in a random deposition. We chose the trial position of particle i given by

$$x_{i,\,trial} = x_i + \Delta x$$
$$y_{i,\,trial} = y_i + \Delta y \qquad (1)$$

The random displacements in vertical and horizontal directions, Δx and Δy, are determined by values chosen within the range of $|\Delta x| \leq \delta$ and $|\Delta y| \leq \delta$,

respectively, where the maximum value of the displacement, δ, is arbitrarily set (here, at 1.0 R_b), where R_b is a reference length, chosen as the radius of one of the particles; the subscript, 'b' stands for 'basis', as mentioned below), depending on the system size, particle size, and so on. If the trial position results in an overlap between particles, it is rejected. Otherwise, the trial position is accepted or rejected according to the transition probability calculated from the change in the potential energy of the system. The transition probability is taken to be

$$P=\exp[-\Delta E/k_BT]=\exp[-Pe\rho^*V^*\Delta y^*], \quad (2)$$

where the dimensionless terms are defined as follows : $Pe=\Delta\rho V_bF_gR_b/k_BT$, $\rho^*=\Delta\rho/\Delta\rho_b$, $\Delta\rho=\rho_p-\rho_m$ $\Delta\rho_b=\rho_b-\rho_m$, $V^*=V/V_b$, and $y^*=y/R_b$, where g is the acceleration due to gravity, F_g is the field strength (=1 for normal gravity), T is the absolute temperature of the system, and k_B is Boltzmann constant. The change of particle position is accepted or rejected according to the resulting transition probability. The above procedure is repeated for each particle, and each such repetition (i.e., for all the N particles) is called a Monte Carlo Step (MCS). The structural features such as the radial distribution functions (defined below) and properties such as the packing and average height are monitored every 100 MCS and the simulation is terminated when these reach asymptotic values.

We have used a much smaller number of particles in these simulations (namely, 150 particles in a strip having a length of 10). The results are based on averages over 10 configurations; this was found to be sufficient for the structural features examined here. Periodic boundary conditions are used in the horizontal direction. Initial volume fraction of particles used in most cases is 0.15, with an initial height of 50. The initial volume fraction of particles can be adjusted by changing either the number of particles or the height of the strip. In what follows, we call the whole region of sediment (i.e., extending from the substrate to the surface) as 'bulk'; the region within ±30 % of the average height is defined as the 'core'. Finally, in the results presented in this work we use a normal field strength of unity, i. e., $F_g=1$.

2.2. Characterization of Structures

The structure of the deposits generated in the simulations is analyzed using diffraction patterns and radial distribution functions of particle positions. For calculating these, only those particles within ±30 % from the mid point are taken so that the influence of the substrate and of the free 'surface' at the top of the packing is avoided. The diffraction patterns are prepared using the structure factor S(q), which is defined by [16]

$$S(q)=(1/M)<|\sum\exp(iq\cdot rj)|^2> \; ; j=1, \cdots, M \quad (3)$$

where rj is the position vector of the j-th particle, the summation is over all M particles in the chosen region, and the bracket <...> denotes the statistical average over the configurations. Broad diffuse haloes in diffraction patterns are observed in the cases of amorphous materials and microcrystalline or nanocrystalline materials.

The radial distribution function, g(r), is a measure of the probability of finding two particles at any center-to-center separation r and is given by

$$g(r)=[\Delta n(r)/2\pi r\Delta r]/\rho_{avg} \quad (4)$$

where $[\Delta n(r)/2\pi r\Delta r]$ is equal to p(r), the local particle density, with $\Delta n(r)$ equal to the number of particles in the interval[r, $r+\Delta r$] and ρ_{avg} is the overall average density of the packing.

The variations of packing fraction, particle number density, average number of contacts, etc., can be studied as functions of the height or as functions of horizontal distance, and the local properties are compared with the bulk properties of the deposits to examine and characterize the structure of the packings.

3. Results and Discussions

A previous work [10] reported that an optimum range of Peclet number for the ordering of sediments exists. This is supported by some experimental results in the literature. Recent experiments [11,12] showed that a crystalline ordering was present in sediments consisting of particles of 200~300 nm in size at initial volume fractions of 0.03 to 0.14. However, such an ordering did not occur in similar suspensions when the particle sizes became larger (> 400 nm). It is noteworthy that the Peclet number is proportional to the fourth power of the particle diameter and increases rapidly with particle size. Thus, the results in Fig. 1 are consistent with the above experimental results.

Figure 2 shows the trajectories of particles starting from different initial positions for different Peclet numbers. An examination of the trajectories of the particles is instructive, since the diffusion of particle and the dynamics of the sediment forma-

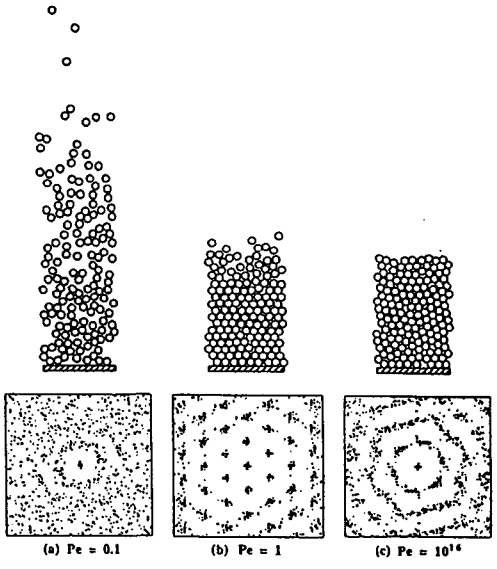

Fig. 1. Structures of the settling suspension and the corresponding diffraction patterns for different Peclet number. (a) Pe $=0.1$, (b) $Pe=1$, and (c) $Pe=10^{16}$.

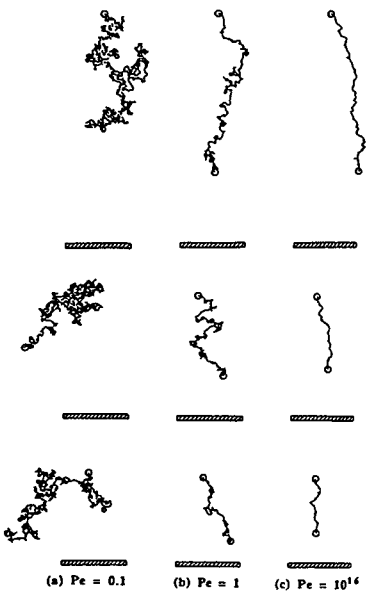

Fig. 2. Trajectories of particles deposited from different heights for different Peclet numbers (a) Pe=0.1, (b) Pe=1, and (c) Pe=10^{16}.

tion are directly related to the trajectories. We observe that, as the Peclet number increases, the trajectory tends to become linear and that the particle travels, on the average, shorter distances before depositing. When the Peclet number is very large, the particulate system is controlled by gravity and the trajectory is expected to show linear paths along the direction of gravity; this is called 'ballistic deposition'. When the Peclet number is very small, the system is controlled by the Brownian force and the trajectory is expected to show random paths; this is often called 'diffusion-limited deposition'. The depth of penetration of the particle can be examined for different Peclet numbers. For Pe =1 a particle can penetrate farther into the sediments and lies at a lower position than in the case of Pe=0.1 and Pe=10^{16}. Thus, computer experimental methods have a distinct advantage over physical experiments and theoretical studies since a trajectory-based analysis is readily accessible.

A typical phase behavior of a dispersion in a sedimentation process as a function of time is shown in Fig. 3 for Pe=1. One notes that the initially well-dispersed particles first settle gradually to form a sediment. Even after a sediment consisting of a 'continuous' phase is formed, rearrange-

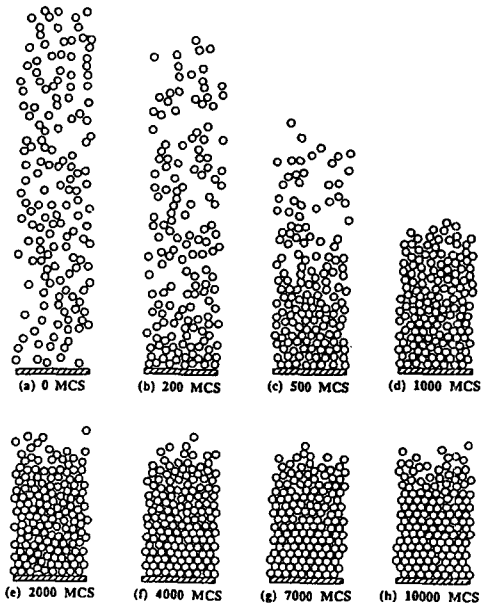

Fig. 3. Structure of the settling suspensions formed at different times for Pe=1 (a) 0 MCS, (b) 200 MCS, (c) 500 MCS, (d) 1,000 MCS, (e) 2,000 MCS, (f) 4,000 MCS, (g) 7,000 MCS, and (h) 10,000 MCS.

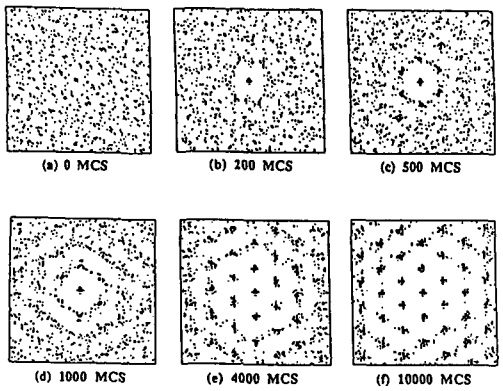

Fig. 4. Radial distribution functions corresponding to the structures shown in Fig. 3 (a) 0 MCS, (b) 1,000 MCS, (c) 2,000 MCS, (d) 4,000 MCS, (e) 7,000 MCS, and (f) 10,000 MCS.

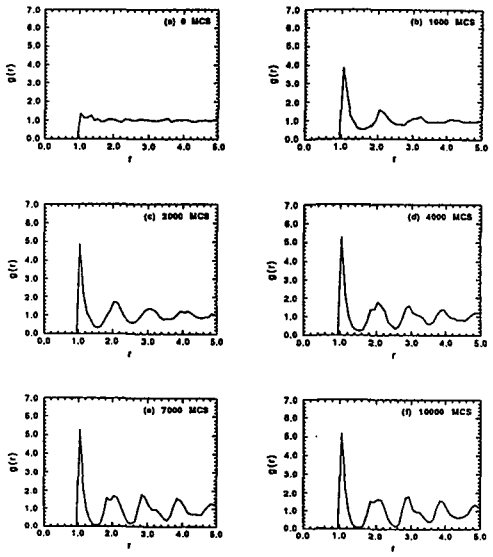

Fig. 5. Diffraction patterns corresponding to the structures shown in Fig. 3 (a) 0 MCS, (b) 1,000 MCS, (c) 2,000 MCS, (d) 4,000 MCS, (e) 7,000 MCS, and (f) 10,000 MCS.

ments of particles in the sediment continue to occur. Figure 4 shows the structural changes in terms of the changes in radial distribution functions at different times. No positional correlation exists among the particles initially (i.e., 0 MCS) since we start with a dispersion containing well-mixed (uniformly distributed) particles (see Fig. 3(a)). As sedimentation proceeds, positional correlations appear locally (i.e., in the neighborhood of the particles) and propagate to longer distances subsequently, as evident from the increasing sharpness of the peaks in the radial distribution functions. Figure 5 shows the corresponding diffraction patterns at various times. One can already see that the structures tend to change gradually from an initial 'gas-like' structure, via an intermediate 'liquid-like' structure, to finally a 'crystal-like' ordered structures as particles sediment. One also finds that the onset of crystallization appears around 4,000 MCS (see Figs. 4(d) and 4(e)). Observation of such an onset of crystallization in experiments has been reported only recently [11]). As seen from Fig. 4, the ordering in the sediment becomes more pronounced with increasing time. However, one should note that the actual phase behavior of the sediments (e.g., whether ordered structures appear in the sediments or not) is determined by the magnitude of the Peclet number, as shown in the previous work [10]).

The packing fraction as a function of depth at different times is shown in Fig. 6. We begin with a suspension containing a uniform distribution of particles at a

low packing fraction of about 0.2. As the particles settle, a 'core' region (as defined in the previous section) with a high packing fraction is formed rapidly. Also we observe that the packing fraction in this core region decreases slightly with increasing height and that, at larger times (e.g., 10,000 MCS), the packing fraction near the substrate decreases slightly from the value in the core region because of boundary effects. These observations, although could not be predicted using currently available theories [15], have been established by recent experimental results in which the variations in Bragg peak positions with height have been obtained from X-ray diffraction [12]. It has been observed in these experiments that there exists an amorphous region at the bottom, below the crystalline region. We note from the gradations in the packing fraction at 500 MCS in Fig. 6 that in general there can exist four different phases (or zones) in the dispersion (with decreasing height) as follows : (i) a clear supernatant phase; (ii) a suspension phase; (iii) a growing surface phase; and (iv) a compact sediment phase. One also note that three interfaces dividing these phases exist. The suspension phase is found only for small Pe. The upper interface is sharp and the lower one consists of an initial jump followed by a compression zone where the packing fraction increases rapidly. Such phases and phase boundaries have been investigated by either (highly simplified, macroscopic) theoretical methods [16,17] or experiments [18]. Figure 7 shows the variation in the structures of

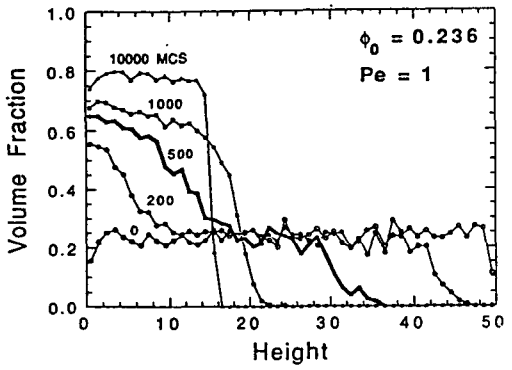

Fig. 6. Packing fraction as a function of the height at different times for Pe=1.

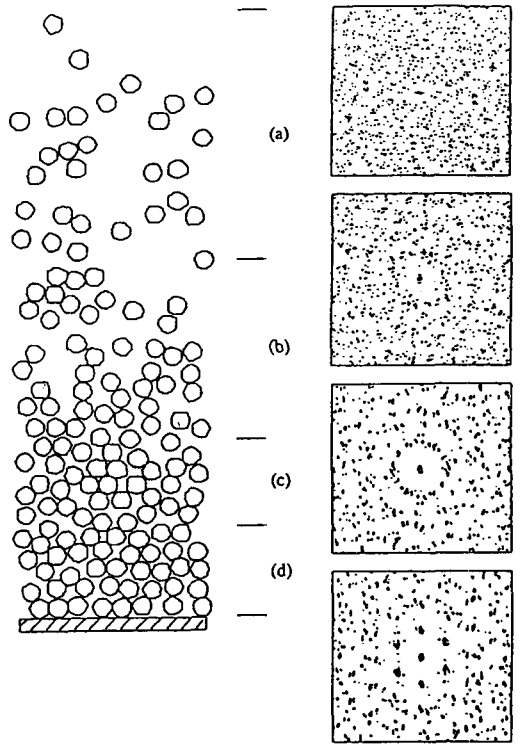

Fig. 7. Structures of different regions observed in a settling suspension at 500 MCS for Pe=1 and diffraction patterns corresponding to the structures.

the deposit as a function of the height and the corresponding diffraction patterns at 500 MCS. As observed previously in Figs. 3~5 in the case of the temporal variation of the phase behavior of the sediments, one again sees that the structures show regions changing from a 'gas-like' structure, via a 'liquid-like' structure, to a 'crystal-like' ordered structures with decreasing height. The diffraction pattern for the near-substrate region shows a clear appearance of hexagonal spots, implying the onset of crystallization (see Fig. 6(d)).

In order to illustrate the effects of the Peclet number and the correlation between the packing fraction and height, the changes in the packing fraction as functions of height and time for Pe=1 and Pe $=10^{16}$ are shown in Fig. 8. The height-versus-time Figs. clearly show the four different phases or regions mentioned earlier. For Pe=1, the supernatant phase, the sediment phase and the coexisting-phase region persist for a long time because of the relative importance of diffusion; however, sedimentation is faster and dominates in the case of large Peclet numbers (e.g., Pe=10^{16}) and one notes that the two-phase region disappears very fast, leaving only the supernatant phase and the sediment phase, with a sharp boundary between the two. Detailed experimental studies of the above variations in packing fractions and the temporal variations of interfaces have only recently begun to appear in the literature [17,18]. It is noteworthy that the region corresponding to the sediment may not necessarily have a crystalline structure.

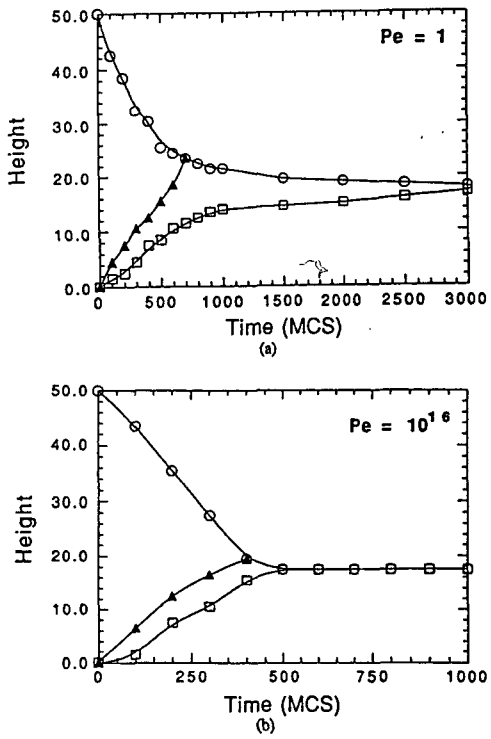

Fig. 8. Trajectory diagrams of the interfaces observed in the settling suspension for (a) Pe=1 and (b) Pe=10^{16}.

Finally, we conclude by emphasizing that the computer simulation method presented here is a good but simple tool which can be used to predict the phase behavior of colloidal dispersions and the resulting microstructure as a function of the relevant physical parameters and to examine and guide experimental studies in advanced ceramic powder processing.

4. Conclusions

We determined the overall structures of monodisperse packings using the magnitude of Peclet number. We showed that the sedimentation led to very compact sediments at a critical value of Peclet number and that the phase structure of the sediments could be determined by the magnitude of Peclet number. Ordered sediments were present only in the Peclet number ranged from 1 to 10. For the particles sediment, the structure near the substrate underwent a phase transition from a gas-like structure to a crystal-like ordered structure, via an intermediate liquid-like structure. A similar phase behavior is also found within the dispersion with decreasing height.

Most studies on packing are restricted in phase structures/transitions (e.g., in physics) or studies on the structural properties of the packing of bulk powders (e. g., in engineering). However, the present work demonstrated that the concept of 'packing phenomena' could apply to a number of packing problems relevant to ceramic powder/film processing such as thin-film vapor deposition, sedimentation of colloid particles, packing of non-Brownian powders.

In summary, this work provides a clue for the understanding of the packing phenomena.

Acknowledgement

This work was supported in part by a Special Fund for University Research Institute, from the Korea Research Foundation.

References

[1] R.J. Pugh and L. Bergstrom, eds., Surface and Colloid Chemistry in Advanced Ceramic Processing (Marcel Dekker, New York, 1994).
[2] F.F. Lange, J. Am. Ceram. Soc. 72 (1989) 3.
[3] E.A. Barringer and H.K. Bowen, J. Am. Ceram. Soc. 65 (1982) C199.
[4] I. Aksay, Ceram. Trans. 1 (1987) 663.
[5] C.S. Hirtzel and R. Rajagopalan, Colloid Phenomena : Advanced Topics (Noyes, Park Ridge, New Jersey, 1985).
[6] P. Pieranski, Am. J. Phys. 52 (1984) 68.
[7] N. Ise and I. Sogami, eds, Ordering and Organisation in Ionic Solutions (World Scientific, Singapore, 1988).
[8] K. Kendall, Powder Technol. 58 (1989) 151.
[9] R.W. Rice, AIChE J. 36 (1990) 481.
[10] H. Kim and R. Rajagopalan, Hwahak Konghak 32 (1994) 659.
[11] S. Emmett, S.D. Lubetkin and B. Vincent, Colloids and Surfaces 43 (1989) 139.
[12] S.D. Lubetkin, D.J. Wedlock and C. F. Edser, Colloids and Surfaces 44 (1990) 139.

[13] W.G. Hoover and F.H. Ree, J. Chem. Phys. 49 (1968) 3609.
[14] L.V. Woodcock, Ann. N. Y. Acad. Sci. 371 (1981) 274.
[15] G.J. Kynch, Trans. Faraday Soc. 48 (1952) 166.
[16] J.P. Hansen and I.R. McDonald, Theory of Simple Liquids, 2nd ed. (Academic Press, New York, 1986).
[17] K.E. Davis and W.B. Russel, Phys. Fluids 82 (1989) A1.
[18] K.E. Davis, W.B. Russel and W.J. Glantschnig, Science 245 (1989) 507.